

# Qubit-mediated energy transfer between thermal reservoirs: beyond Markovian Master equation

Dvira Segal

*Chemical Physics Theory Group, Department of Chemistry,  
University of Toronto, 80 Saint George St. Toronto, Ontario, Canada M5S 3H6*  
(Dated: March 26, 2013)

We study qubit-mediated energy transfer between two electron reservoirs by adopting a numerically-exact influence functional path-integral method. This non-perturbative technique allows us to study the system's dynamics beyond the weak coupling limit. Our simulations for the energy current indicate that perturbative-Markovian Master equation predictions significantly deviate from exact numerical results already at intermediate coupling,  $\pi\rho\alpha_{j,j'} \gtrsim 0.4$ , where  $\rho$  is the metal (Fermi sea) density of states, taken as a constant, and  $\alpha_{j,j'}$  is the scattering potential energy of electrons, between the  $j$  and  $j'$  states. Markovian Master equation techniques should be therefore used with caution beyond the strictly weak subsystem-bath coupling limit, especially when a quantitative knowledge of transport characteristics is desired.

PACS numbers: 05.60.-k, 44.10.+i, 44.40.+a, 73.23.-b

## I. INTRODUCTION

Quantum impurity models, including a subsystem interacting with a reservoir, were proven useful in describing and predicting many physical phenomena. The spin-boson model [1], representing the dynamics of a single charge on two states coupled to a dissipative bath, e.g., a solvent, exhibits rich phenomenology, including various phase transitions [2]. It is relevant for modeling charge transfer reactions in biological systems [2], photosynthesis [3], the Kondo problem for magnetic impurities [4], and quantum information processing in superconducting Josephson tunneling junction qubits [5] or nitrogen-vacancy centers in diamonds [6]. A variant of the spin-boson model is the spin-fermion model, where a qubit, referred to as a spin or a two-level system, interacts with a metallic-fermionic environment. This model is also related to the Kondo model [4], only lacking direct coupling of the reservoir degrees of freedom to spin-flip processes. The generalization of the equilibrium spin-fermion model, to include more than one Fermi bath, provides a minimal setting for the study of dissipation and decoherence effects under the influence of an out-of-equilibrium environment [7–10].

In this work, we use the two-bath spin-fermion model and investigate energy exchange between two metals, mediated by the excitation/relaxation of a nonlinear quantum system, a qubit. For a scheme of this setup, see Fig. 1. Physically, our model can describe the process of radiative heat transfer between metals [11–13], and it can be realized within a superconducting Josephson junction circuit [10, 14, 15]. We simulate the energy current characteristics of the nonequilibrium spin-fermion model in a large parameter range of coupling strengths by means of an influence-functional path-integral (INFPI) technique developed in Refs. [16, 17]. This numerically-exact method is built about the basic observation, that in out-of-equilibrium (and/or finite temperature) situations bath correlations have a finite range, allowing

for their truncation beyond a memory time dictated by the voltage-bias and the temperature [8, 9, 18]. Taking advantage of this fact, an iterative-deterministic time-evolution scheme can be developed, where convergence with respect to the memory length can in principle be reached.

Our main objective here is to explore the qubit-mediated energy current characteristics beyond standard perturbative methods. Particularly, we would like to find when the Golden-Rule-type Markovian Master equation method provides a correct (quantitative or qualitative) description of the exact behavior. This task is important since Master equation tools have been extensively adopted for studying problems in charge, spin, and energy transfer phenomenology in quantum dots and molecular junctions, see for example [13, 19–28].

The plan of the paper is as follows. In Sec. II we present the nonequilibrium spin-fermion model. We provide expressions for observables of interest in Sec. III. The two methods confronted, INFPI and Markovian Master equation, are discussed in Sec. IV, with results included in Sec. V. Sec. VI concludes. For simplicity, we use the conventions  $\hbar \equiv 1$ , electron charge  $e \equiv 1$ , and Boltzmann constant  $k_B = 1$ .

## II. MODEL

The system of interest comprises of two metallic leads,  $\nu = L, R$ , prepared at different temperatures but at the same chemical potential. These metals are connected indirectly, by a nonlinear quantum unit, a two-level subsystem. The Hamiltonian includes three contributions,

$$H = H_S + H_F + V, \quad (1)$$

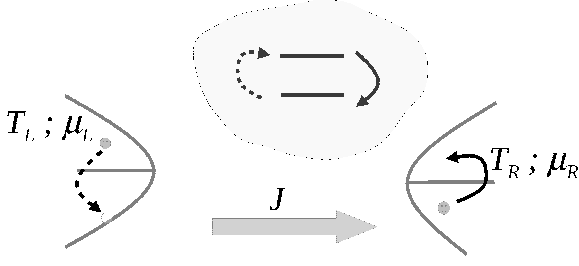


FIG. 1. A schematic representation of our model system. Electron transfer between the metals is blocked, but energy current is flowing through an excitation/de-excitation of the intermediate anharmonic (two-state) quantum system. The curved arrows represent energy transfer processes between the leads and the intermediating subsystem. In our work here we set  $\mu_L = \mu_R$  and take  $T_L > T_R$ .

where

$$\begin{aligned} H_S &= \Delta \sigma_z, \\ H_F &= H_L + H_R, \quad H_\nu = \sum_{j \in \nu} \epsilon_j c_{\nu,j}^\dagger c_{\nu,j} \\ V &= V_L + V_R, \quad V_\nu = \sigma_x \sum_{j,j'} \alpha_{\nu,j;\nu,j'} c_{\nu,j}^\dagger c_{\nu,j'}. \end{aligned} \quad (2)$$

The subsystem  $H_S$  includes two states,  $|0\rangle$  and  $|1\rangle$ , with a tunneling splitting  $2\Delta$ . It can be realized within a nonlinear resonator mode, or it can represent an impurity in a solid-state environment. This subsystem interacts with two fermionic reservoirs ( $H_F$ ) where  $c_{\nu,j}^\dagger$  ( $c_{\nu,j}$ ) creates (annihilates) an electron at the  $\nu = L, R$  metal lead with momentum  $j$ , disregarding the electron spin degree of freedom. The qubit-metal interaction term  $V$  couples scattering events within each metal to transitions within the subsystem. For simplicity, we assume that the coupling constants  $\alpha_\nu$  are energy independent and real numbers. Note that we do not allow for charge transfer processes between the two metals, assuming the tunneling barrier is high. However, energy is transferred between the two metals, mediated by the excitation of the intermediate nonlinear quantum system, see Fig. 1. Using the Hamiltonian form (2), the subsystem dynamics and the energy current can be readily attained within a Markovian Master equation, as we explain in Sec. IV.B

The Hamiltonian (2) can be transformed into the standard spin-fermion model of zero energy spacing with a unitary transformation,

$$U^\dagger \sigma_z U = \sigma_x, \quad U^\dagger \sigma_x U = \sigma_z, \quad (3)$$

where  $U = \frac{1}{\sqrt{2}}(\sigma_x + \sigma_z)$ . The transformed Hamiltonian  $H_{SF} = U^\dagger H U$  includes a  $\sigma_z$ -type electron-spin coupling,

$$\begin{aligned} H_{SF} &= \Delta \sigma_x + \sum_{\nu,j} \epsilon_j c_{\nu,j}^\dagger c_{\nu,j} \\ &+ \sigma_z \sum_{\nu,j,j'} \alpha_{\nu,j;\nu,j'} c_{\nu,j}^\dagger c_{\nu,j'}. \end{aligned} \quad (4)$$

In this representation, the dynamics can be conveniently simulated with INFPI, a brief discussion is included in Sec. IV.A.

### III. OBSERVABLES

We assume a factorized initial state with the total density matrix  $\rho(0) = \rho_S(0) \otimes \rho_F$ . Here  $\rho_S$  denotes the reduced density matrix of the subsystem. The reservoirs' density matrix at time  $t = 0$  is given by  $\rho_F = \rho_L \otimes \rho_R$ , and these states are canonical,  $\rho_\nu = e^{-\beta_\nu(H_\nu - \mu_\nu N_\nu)} / \text{Tr}_\nu[e^{-\beta_\nu(H_\nu - \mu_\nu N_\nu)}]$ . Here we trace over the  $\nu$  reservoirs degrees of freedom. In our simulations below we take  $\mu_L = \mu_R$ , but assume different initial temperatures,  $T_L \neq T_R$ . We refer to this setup as a “nonequilibrium environment” since the two reservoirs are prepared in different states. At time  $t = 0$  we put into contact the two Fermi baths through the quantum subsystem, and follow the evolution of the reduced density matrix and the energy current, to steady-state. Since the energy current in the system is driven by a temperature bias, we can also refer to the energy current here as a “heat current”.

The time evolution of the reduced density matrix is obtained by tracing  $\rho$  over the fermionic reservoirs' degrees of freedom,

$$\rho_S(t) = \text{Tr}_F [e^{-iHt} \rho(0) e^{iHt}]. \quad (5)$$

The definition of the energy current operator is more subtle [29, 30], as different-plausible choices provide distinct results in the short time limit. At long time, in the steady-state limit, these definitions yield the same value. Here, we follow the analysis of Ref. [29], and define the energy current operator, e.g., at the left contact, as

$$\hat{J}_\nu = \frac{i}{2} [H_L - H_S, V_L]. \quad (6)$$

In steady-state the expectation value of the interaction is zero, and we reach the relation,

$$\text{Tr} \left[ \rho \frac{\partial V_L}{\partial t} \right] \equiv \left\langle \frac{\partial V_L}{\partial t} \right\rangle = i \langle [H_S + H_L, V_L] \rangle = 0. \quad (7)$$

Note that we have assumed that  $[V_L, V_R] = 0$ . Using Eq. (7) we reach the following expression for the averaged energy current (valid in the long time limit),

$$\langle J_L \rangle \equiv \text{Tr}_S \text{Tr}_F [\hat{J}_L \rho(t)] = -i \langle [H_S, V_L] \rangle. \quad (8)$$

This commutator can be readily evaluated to yield,

$$[H_S, V_L] = 2i\Delta\sigma_y \sum_{l,l'} \alpha_{L,l;L,l'} c_{L,l}^\dagger c_{L,l'}, \quad (9)$$

leading to

$$\langle J_L \rangle = 2\Delta \text{Tr}_S [\sigma_y \text{Tr}_F [A_L \rho(t)]] , \quad (10)$$

with the bath operator  $A_L \equiv \sum_{l,l'} \alpha_{L,l;l,l'} c_{L,l}^\dagger c_{L,l'}$ . We now define a subsystem operator

$$A_S(t) \equiv \text{Tr}_F[A_L \rho(t)] = \text{Tr}_F[e^{iHt} A_L e^{-iHt} \rho(0)], \quad (11)$$

and express the current using its matrix elements

$$\langle J_L \rangle = 2\Delta[-i(A_S(t))_{1,0} + i(A_S(t))_{0,1}]. \quad (12)$$

We emphasize that this expression is designed to provide the steady-state value and not the transients, given our assumption (7).

The two operators,  $\rho_S(t)$  and  $A_S(t)$ , are subsystem operators. They are simulated in the next section directly, using INFPI, or studied in a perturbative manner, under the Markovian limit, to provide Kinetic-type expressions.

## IV. METHODS

### A. Path-integral simulations

The principles of the INFPI approach have been detailed in Refs. [16, 17], where it has been adopted for investigating dissipation effects in the nonequilibrium spin-fermion model and charge occupation dynamics in the interacting Anderson model. Other applications include the study of the intrinsic coherence dynamics in a double quantum dot Aharonov-Bohm interferometer [31], exploration of relaxation and equilibration dynamics in finite metal grains [32], and the study of electron-phonon effects in molecular rectifiers [33].

Here, using INFPI, we can directly simulate both the dynamics of the reduced density matrix  $\rho_S(t)$  [Eq. (5)], and the time evolution of subsystem expectation values, particularly  $A_S(t)$  [Eq. (11)], which can be used to obtain the energy current  $\langle J_L \rangle$ , Eq. (12). In practice, for achieving fast convergence, we have simulated directly the averaged current

$$J = \frac{1}{2}(\langle J_L \rangle - \langle J_R \rangle). \quad (13)$$

The negative sign in front of  $\langle J_R \rangle$  arises from our sign convention; the current  $\langle J_\nu \rangle$  is defined from the  $\nu$  reservoir, into the junction.

Algorithmic details of the INFPI method were recently elaborated in Ref. [33], thus we only include the main principles here. The algorithm is based on a Trotter breakup of a short-time time evolution operator into two parts: a (simple) time evolution term that depends on the subsystem Hamiltonian, and a term that accommodates the reservoirs Hamiltonians, and their interactions with the subsystem. Collecting the contribution of the latter terms along the subsystem path, we construct the so called “influence functional” (IF), which involves non-local dynamical correlations. The IF has an analytical form in some special cases [18]; in the present model its form is only known in the weak-intermediate coupling limit [8, 9], thus we evaluate it numerically by energy-discretizing the Fermi sea.

The main conceptual element behind the INFPI approach is the observation that at finite temperatures and/or nonzero chemical potential bias bath correlations exponentially decay in time, allowing for their truncation beyond a memory time  $\tau_c$ . The dynamics can then be achieved by defining an auxiliary density matrix, or more generally, a subsystem operator [e.g.,  $A_S(t)$  of Eq. (11)], on the time-window  $\tau_c$ . This nonlocal object can be iteratively evolved from the subsystem-bath factorized initial condition, to the present time  $t$ .

This path-integral method involves three numerical parameters: (i) the number of states used in the discretization of each Fermi sea  $L$ , (ii) the time step adopted in the Trotter breakup  $\delta t$ , and (iii) the memory time accounted for,  $\tau_c$ , beyond which the IF, accommodating the effect of the reservoirs on the subsystem, is truncated. Convergence of INFPI is verified by confirming that results are insensitive to the reservoirs discretization, the finiteness of the time step, and the memory size  $\tau_c = N_s \delta t$ , with  $N_s$  as an integer. It should be noted that minimizing the Trotter breakup error, taking  $\delta t \rightarrow 0$ , conflicts with the need to cover the memory time-window  $\tau_c$ , since the parameter  $N_s$  has to be increased until convergence is reached. Since our computational effort scales as  $d^{2N_s}$ , where  $d$  is the Hilbert space dimensionality of the subsystem, we are practically limited to  $N_s < 10$ , implying on the minimal time step that can be adopted.

### B. Markovian Master Equation

The dynamics of the model (2), and its variants, can be analyzed in the weak subsystem-bath coupling limit under the Markovian approximation [13, 34]. The probabilities  $P_n$  to occupy the  $|n\rangle$  state of the subsystem, the quantum impurity, satisfy the Master equation

$$\dot{P}_n = \sum_m P_m k_{m \rightarrow n} - P_n \sum_m k_{n \rightarrow m}, \quad (14)$$

where the transition rate from the state  $|m\rangle$  to  $|n\rangle$  ( $m \neq n$  and  $m, n=0,1$  here) is additive in the  $L$  and  $R$  reservoirs,  $k_{n \rightarrow m} = k_{n \rightarrow m}^L + k_{n \rightarrow m}^R$ , due to the linear form of the interaction [21, 35].

This type of Kinetic equation has been used in many recent works for investigating energy, spin, and charge transfer in open quantum systems [20, 21]. Particularly, it has been recently adopted for modeling radiative energy transfer between metals [13, 28], and for studying charge and energy transfer phenomenology in mesoscopic systems [19, 22, 24, 25] and single molecules [23]. It is thus important to test the suitability and accuracy of this common and well-accepted approximate scheme against exact results.

In steady-state, taking Eq. (12) as a starting point, one can show that in the weak coupling limit and under the Markovian approximation the energy current across

the system reduces to [29] ( $\langle J_L \rangle = J$  in steady-state),

$$J = \sum_{m,n} E_{m,n} P_n k_{n \rightarrow m}^L, \quad (15)$$

with  $E_{m,n} = E_m - E_n$ . The current is defined positive when flowing left to right. At the level of the Golden-Rule formula, the transition rates are given by [13]

$$\begin{aligned} k_{n \rightarrow m}^\nu &= 2\pi \sum_{j,j'} |\alpha_{\nu,j;\nu,j'}|^2 n_F^\nu(\epsilon_k) [1 - n_F^\nu(\epsilon_{j'})] \delta(\epsilon_j - \epsilon_{j'} - E_{m,n}) \\ &= 2\pi \int d\epsilon n_F^\nu(\epsilon) [1 - n_F^\nu(\epsilon - E_{m,n})] F_\nu(\epsilon). \\ &= -2\pi n_B^\nu(E_{m,n}) \int d\epsilon [n_F^\nu(\epsilon) - n_F^\nu(\epsilon - E_{m,n})] F_\nu(\epsilon) \end{aligned} \quad (16)$$

From the last relation we note that the thermal properties of the reservoirs are concealed within both the Fermi-Dirac distribution function  $n_F^\nu(\epsilon) = [e^{(\epsilon - \mu_\nu)/T_\nu} + 1]^{-1}$  and the Bose-Einstein occupation factor  $n_B^\nu(\epsilon) = [e^{\epsilon/T_\nu} - 1]^{-1}$ . It is therefore clear that when the integral yields a temperature independent constant, the statistic of the reservoirs is fully bosonic [13]. The other element in Eq. (16) is a dimensionless interaction term

$$F_\nu(\epsilon) = |\alpha_\nu|^2 \rho_\nu(\epsilon) \rho_\nu(\epsilon - E_{m,n}), \quad (17)$$

which encloses the properties of the reservoirs, multiplied by the subsystem-bath (energy independent) couplings  $\alpha_\nu$ . Once we assume that the density of states is a constant [36],  $F_\nu(\epsilon) \approx F_\nu(\mu_\nu)$ , the integration in Eq. (16) can be performed when the Fermi energies are situated far from the conduction band edges [36]. Making use of the following relation,

$$\int_{-\infty}^{\infty} d\epsilon [n_F^\nu(\epsilon) - n_F^\nu(\epsilon - E_{m,n})] = -E_{m,n}, \quad (18)$$

we reach the closed-form expression,

$$k_{n \rightarrow m}^\nu = 2\pi n_B^\nu(E_{m,n}) E_{m,n} F_\nu(\mu_\nu). \quad (19)$$

Note that  $n_B(-E_{m,n}) = -[n_B(E_{m,n}) + 1]$ , thus the excitation and relaxation rates induced by the  $\nu$  reservoir satisfy the detailed balance relation,  $k_{n \rightarrow m}^\nu / k_{m \rightarrow n}^\nu = e^{-E_{m,n}/T_\nu}$ . We can also express the rates in terms of a subsystem-bath interaction parameter

$$\Gamma_F^\nu(2\Delta) \equiv 2\pi F_\nu(\mu_\nu) 2\Delta = 2 \frac{2\Delta}{\pi} [\pi \rho_\nu(\mu_\nu) \alpha_\nu]^2, \quad (20)$$

where we recall that both the density of states and the interaction parameter  $\alpha$  are assumed to be energy independent. Using this defining, the rate constants in our model reduce to

$$\begin{aligned} k_{1 \rightarrow 0}^\nu &= \Gamma_F^\nu(2\Delta) [1 + n_B^\nu(2\Delta)], \\ k_{0 \rightarrow 1}^\nu &= \Gamma_F^\nu(2\Delta) n_B^\nu(2\Delta). \end{aligned} \quad (21)$$

For simplicity, we do not include below the explicit dependence of  $\Gamma_F^\nu$  and  $n_B^\nu$  on energy; both quantities should

be evaluated at the subsystem energy gap  $2\Delta$ . We calculate the population of the states in steady-state by putting  $\dot{P}_n = 0$  in Eq. (14). With this at hand, the energy current (15) simplifies to [37]

$$J = 2\Delta \frac{\Gamma_F^L \Gamma_F^R [n_B^L - n_B^R]}{\Gamma_F^L (1 + 2n_B^L) + \Gamma_F^R (1 + 2n_B^R)}. \quad (22)$$

This expression provides the steady-state energy current in the weak coupling limit, under the Markovian approximation.

It should be noted that a more involved non-interacting blip-approximation (NIBA) type scheme [1] can be implemented for following the qubit dynamics in the nonequilibrium spin-fermion model [7]. Furthermore, besides the qubit dynamics itself, the heat current can be simulated within the NIBA approximation by extending a generating function technique developed in Ref. [38] for the study of transport behavior in the nonequilibrium spin-boson model. However, here we contain ourselves with the simpler, more standard and common Markovian Master equation, with the objective to provide insight on its applicability and accuracy for the large community adopting it in studies of charge, spin, and energy dynamics in mesoscopic and molecular systems.

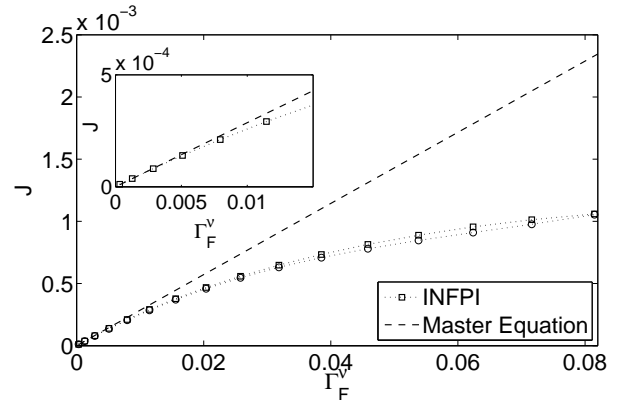


FIG. 2. Energy current as a function of metal-qubit coupling parameter  $\Gamma_F^\nu$  using the bandwidth  $D = 2$ ,  $\Delta = 0.1$ ,  $T_L = 0.4$ , and  $T_R = 0.2$ . INFPI numerical parameters are  $\delta t = 1$  and  $N_s = 9$ . Dashed line: Master equation results. INFPI results appear in symbols,  $\square$  for  $L = 40$  and  $\circ$  when taking the asymptotic  $L \rightarrow \infty$  limit. Inset: Zooming over the small coupling limit where the current linearly scales with  $\Gamma_F^\nu$ .

## V. RESULTS

We compare INFPI simulations to the Master equation predictions. Within INFPI, the current is simulated directly using Eqs. (11) and (12), and we show results only in the long time (quasi) steady-state limit. The closed-form Master equation expression is given by (22). Beyond the weak coupling limit, we calculate the Master equation current directly from Eq. (15) using the rates

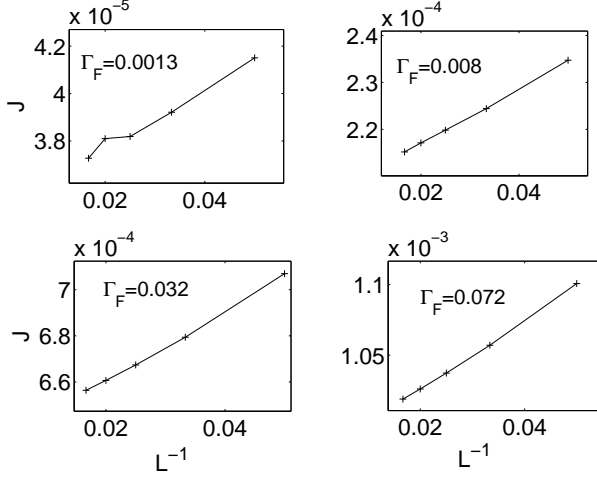


FIG. 3. Converging the data of Fig. 2 to the  $L^{-1} \rightarrow 0$  limit, with the intercept representing the asymptotic result.

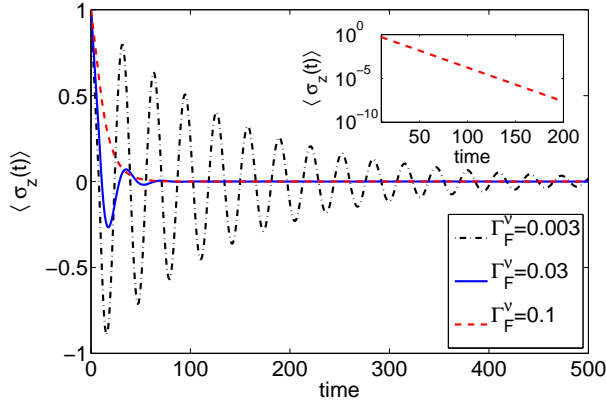


FIG. 4. Polarization dynamics at different coupling strengths, for the same set of parameter as in Fig. 2. Results are displayed in the basis of the Hamiltonian (4)

(16), since the wide-band approximation does not hold anymore (though of course the applicability of the Master equation technique as a whole is questionable in this regime).

We typically use the following set of parameters: an energy gap  $2\Delta = 0.2$  (arbitrary units) for the subsystem, metallic bandwidth  $D = 2$ ,  $T_\nu \gtrsim \Delta$ , and the equilibrium Fermi energies located at the center of the band. We also define the dimensionless parameter

$$\phi_\nu = \pi \rho_\nu \alpha_\nu, \quad (23)$$

which is varied between 0 and 0.8 here, where convergence is achieved. This choice corresponds to  $0 < \Gamma_F^\nu < 0.08$  when  $\Delta = 0.1$ , see Eq. (20). For this set of model parameters, we have confirmed that selecting  $\delta t = 0.8 - 1.5$  and  $N_s = 6 - 9$  (yielding memory time  $\tau_c \geq 8$ ) provides converging results, see panel b in Figs. 5, 6 and 7.

Before turning to simulations, it is important to identify the region of weak subsystem-bath coupling. It holds

when the scattering phase shift is small,  $\arctan \phi_\nu \sim \phi_\nu$  [39]. This translates (within 5% error) to the dimensionless parameter  $\phi$  being limited to the domain of  $\phi_\nu \lesssim 0.4$ . Equivalently, the interaction energy should be limited to  $\Gamma_F^\nu \lesssim 0.02$ , or in other words,  $\Gamma_F^\nu/(2\Delta) \lesssim 0.1$ , i.e., in the weak coupling limit the subsystem gap is large relative to the coupling energy.

Fig. 2 displays the energy current as a function of the interaction energy for a symmetric junction,  $\Gamma_F^L = \Gamma_F^R$ . We find that when  $\Gamma_F^\nu \gtrsim 0.02$ , Master equation-derived energy current overestimates the exact result by more than 10%. In the strong coupling limit, Master equation overvalues the correct numbers by a factor of two. More significantly, this Golden-Rule based method cannot reproduce the saturation effect of the current with the subsystem-bath interaction parameter, and it wrongly predicts a linear scaling,  $J \propto \Gamma_F^\nu$ . Note that we include INFPI results both for the case of  $L = 40$  bath states ( $\square$ ), and in the asymptotic  $L \rightarrow \infty$  limit ( $\circ$ ), obtained by extrapolating the linear  $J$  vs.  $L^{-1}$  curves to  $L^{-1} \rightarrow 0$ , see Fig. 3. We find that this extrapolation affects the results by up to 4% at strong coupling, while the weak coupling values are unaffected. While we do not show transient data for the current, we comment that steady-state has been reached at  $\Delta t \sim 50 - 100$  in the weak coupling limit; it is established much faster,  $\Delta t \sim 5 - 10$  at strong coupling.

We correlate transport behavior of the junction with a study of the dissipative dynamics of the spin polarization, as obtained from INFPI, in Fig. 4. We observe weakly-damped coherent oscillations in the weak coupling limit when perturbative Master equation well describes the dynamics. These oscillations still survive at intermediate coupling, but at strong coupling the polarization exponentially decays in time (inset). Crucial parameters of the model are the scattering phase shifts  $\delta_\pm$ . In equilibrium, the phase shifts are given by [39, 40]

$$\tan \delta_\pm = \phi_{L,R} \quad (24)$$

Out-of-equilibrium,  $\Delta\mu \neq 0$ , the phase shifts are *complex* numbers [40]. In the spin-boson model the Kondo dimensionless dissipation coefficient  $\xi$  represents a characteristic exponent in the system: at zero temperature and zero energy bias the spin displays damped coherent oscillations for  $\xi < 0.5$ , relaxation dynamics between  $0.5 \leq \xi < 1$ , and a localization phase for  $\xi \geq 1$  [41]. Thus, this parameter controls dissipation-induced phase transitions. In the fermionic analogue it can be shown that the characteristic exponent is given by  $\xi = (\delta_+^2 + \delta_-^2)/\pi^2$  [40]. Since  $|\delta_\pm| \leq \pi/2$ ,  $\xi \leq 1/2$ . Thus, in the spin-fermion model described in this paper the spin cannot manifest the localization behavior, and a large  $\phi$  value brings us to the relaxation scenario, as indeed observed in Fig. 4.

The current-temperature characteristics of the junction are depicted in Figs. 5-7, using different coupling strengths. We find that at weak coupling Markovian Master equation very well reproduces the qualitative and

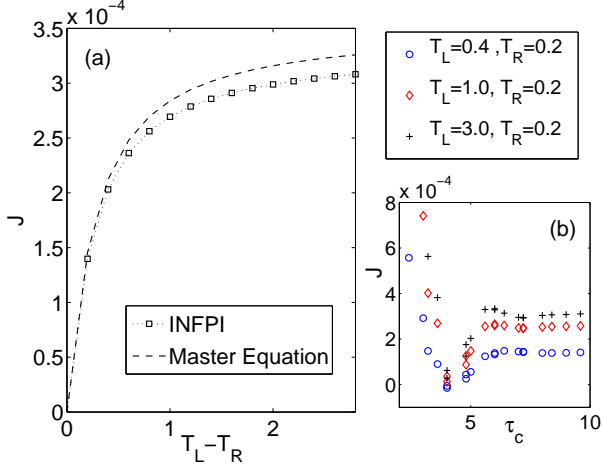


FIG. 5. (a) Energy current-temperature characteristics for the same set of parameter as in Fig. 2,  $\phi = 0.2$  ( $\Gamma_F = 0.005$ ). We vary  $T_L$ , but keep  $T_R$  fixed,  $T_R = 0.2$ . (b) Convergence behavior with increasing memory size. Data was produced with three different time steps,  $\delta t = 0.8, 1.0$  and  $1.2$ .

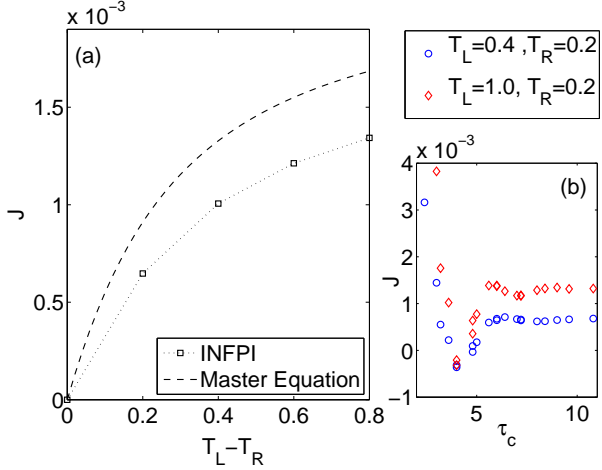


FIG. 6. (a) Energy current-temperature characteristics for the same set of parameter as in Fig. 2,  $\phi = 0.5$  ( $\Gamma_F = 0.032$ ). We vary  $T_L$ , but keep  $T_R$  fixed,  $T_R = 0.2$ . (b) Convergence behavior with increasing memory size. Data was produced with three different time steps,  $\delta t = 0.8, 1.0$  and  $1.2$ .

quantitative aspects of the current, even at a large temperature difference, see Fig. 5. The convergence behavior of the INFPPI method at different temperature biases is displayed in panel (b), where we show the energy current as obtained using different memory time  $\tau_c$  and time steps. At intermediate couplings, Fig. 6 shows that Master equation overestimates exact results by up to 25% at large temperature differences. When the subsystem-bath coupling is large, we managed to converge simulations only up to the bias  $T_L - T_R \sim 0.2$ . The Kinetic method now provides values that are a factor of 2 larger than the exact numerical data. It is important to note that the qualitative current-temperature features are correctly re-

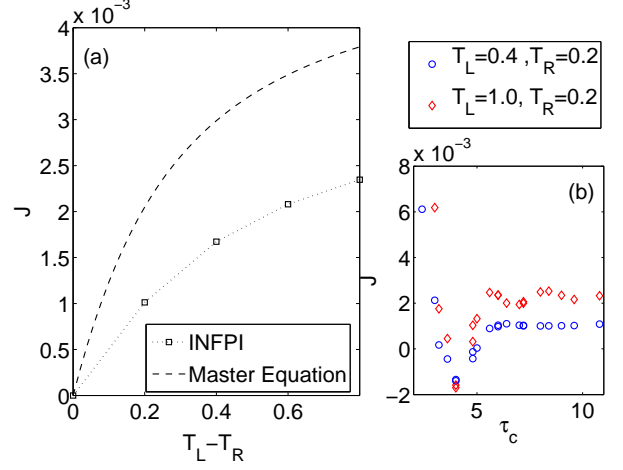


FIG. 7. (a) Energy current-temperature characteristics for the same set of parameter as in Fig. 2,  $\phi = 0.75$  ( $\Gamma_F = 0.072$ ). We vary  $T_L$ , but keep  $T_R$  fixed,  $T_R = 0.2$ . (b) Convergence behavior with increasing memory size: results converge only at small bias,  $T_L - T_R < 0.4$ . Data was produced with three different time steps,  $\delta t = 0.8, 1.0$  and  $1.2$ .

produced within the Markovian Master equation, even at strong coupling. However, if one is interested in quantitative information, Master equation can be used in its strict regime of applicability only,  $\phi \lesssim 0.2$ . Data in Figs. 5-7 is presented for a fixed value of bath states,  $L = 40$ , since we have confirmed that taking the large- $L$  limit only corrects the current by  $\lesssim 4\%$ , at both low and high temperature biases.

## VI. SUMMARY

We have studied energy transfer between metals mediated by a quantum impurity, using two approaches: numerically exact path-integral simulations and analytic results from a Golden-Rule type Markovian Master equation treatment. We found that standard Master equations fail to reproduce the current-interaction energy characteristics already at intermediate system-bath couplings, as it can only provide a linear enhancement of the current with the subsystem-bath interaction, missing a saturation effect. In contrast, the current-temperature characteristics is produced in a qualitative correct way by a Master equation formalism, though actual values deviate by 100%, and more, at high temperature biases and at strong coupling.

Our results are beneficial for the critical testing of common Master equation techniques. The methods described are also useful for practically modeling superconducting-based qubit devices [42]. While a Master equation treatment offers simple-intuitive expressions that often allow to discern essential transport characteristics, already at intermediate system-bath couplings it may overestimate the current by  $\sim 10\%$ , up to a 100% incorrect enhance-

ment at strong coupling. These deviations are certainly important when a quantitative analysis of device efficiency is performed. In particular, the calculation of energy conversion efficiency in conducting junctions should be done with caution when a Master equation is of use [22, 26, 43].

In our future work we plan to study the heat current characteristics in the complementary spin-boson type molecular junction model [37]. This could be done by extending the Feynman-Vernon IF expression [44] to describe the evolution of other operators besides the re-

duced density matrix. Alternatively, one could use the bosonization approach and draw general results for the nonequilibrium spin-boson problem, based on the spin-fermion model calculations presented here.

## ACKNOWLEDGMENTS

Support from an NSERC discovery grant is acknowledged.

- 
- [1] A. J. Leggett, S. Chakravarty, A. T. Dorsey, M. P. A. Fisher, A. Garg, and W. Zwerger, *Rev. Mod. Phys.* **59**, 1 (1987).
  - [2] U. Weiss, *Quantum Dissipative Systems* (World Scientific, 1993).
  - [3] J. Gilmore and R. McKenzie, *J. Phys.: Cond. Matt.* **17**, 1735 (2005).
  - [4] J. Kondo, *Prog. Theor. Phys.* **32**, 37 (1964).
  - [5] Y. Makhlin, G. Schon, and A. Shnirman, *Rev. Mod. Phys.* **73**, 357 (2001).
  - [6] G. D. Fuchs, G. Burkard, P. V. Klimov, and D. D. Awschalom, *Nature* **7**, 789 (2011).
  - [7] A. Mitra and A. J. Millis, *Phys. Rev. B* **72**, 121102(R) (2005).
  - [8] A. Mitra and A. J. Millis, *Phys. Rev. B* **76**, 085342 (2007).
  - [9] D. Segal, D. R. Reichman, and A. J. Millis, *Phys. Rev. B* **76**, 195316 (2007).
  - [10] R. M. Lutchyn, L. Cywinski, C. P. Nave, and S. D. Sarma, *Phys. Rev. B* **78**, 024508 (2008).
  - [11] M. Meschke, W. Guichard, and J. P. Pekola, *Science* **444**, 187 (2006).
  - [12] J. P. Pekola and F. W. J. Hekking, *Phys. Rev. Lett.* **98**, 210604 (2007).
  - [13] D. Segal, *Phys. Rev. Lett.* **100**, 105901 (2008).
  - [14] T. Ruokola, T. Ojanen, and A.-P. Jauho, *Phys. Rev. B* **79**, 144306 (2009).
  - [15] J. Koch, T. M. Yu, J. Gambetta, A. A. Houck, D. I. Schuster, J. Majer, A. Blais, M. H. Devoret, S. M. Girvin, and R. J. Schoelkopf, *Phys. Rev. A* **76**, 042319 (2007).
  - [16] D. Segal, A. J. Millis, and D. R. Reichman, *Phys. Rev. B* **82**, 205323 (2010).
  - [17] D. Segal, A. J. Millis, and D. R. Reichman, *Phys. Chem. Chem. Phys.* **13**, 14378 (2011).
  - [18] N. Makri, *J. Math. Phys.* **36**, 2430 (1995).
  - [19] T. Brandes, *Phys. Rep.* **408**, 315 (2005).
  - [20] A. Mitra, I. Aleiner, and A. J. Millis, *Phys. Rev. B* **69**, 245302 (2004).
  - [21] L.-A. Wu, C. X. Yu, and D. Segal, *Phys. Rev. E* **80**, 041103 (2009).
  - [22] G. Schaller, C. Emary, G. Kiesslich, and T. Brandes, *Phys. Rev. B* **84**, 085418 (2005).
  - [23] J. Koch, F. von Oppen, Y. Oreg, and E. Sela, *Phys. Rev. B* **70**, 195107 (2004); J. Koch and F. von Oppen, *Phys. Rev. Lett.* **94**, 206804 (2005); J. Koch, M. E. Raikh, and F. von Oppen, *ibid.* **96**, 056803 (2006); J. Koch, M. Semmelhack, F. von Oppen, and A. Nitzan, *Phys. Rev. B* **73**, 155306 (2006).
  - [24] T. Ojanen, *Phys. Rev. B* **80**, 180301 (2009).
  - [25] T. Ruokola and T. Ojanen, *Phys. Rev. B* **83**, 241404 (2011).
  - [26] T. Ruokola and T. Ojanen, *Phys. Rev. B* **86**, 035454 (2012).
  - [27] G. Schaller, *Phys. Rev. E* **83**, 031111 (2011).
  - [28] P. J. Jones, J. A. M. Huhtamaki, K. Y. Tan, and M. Mottonen, *Phys. Rev. B* **85**, 075413 (2012).
  - [29] L.-A. Wu and D. Segal, *J. Phys. A: Math. and Theo.* **42**, 025302 (2009).
  - [30] K. Velizhanin, H. Wang, and M. Thoss, *Chem. Phys. Lett.* **460**, 325 (2008).
  - [31] S. Bedkhal and D. Segal, *Phys. Rev. B* **85**, 155324 (2012).
  - [32] M. Kulkarni, K. L. Tiwari, and D. Segal, *Phys. Rev. B* **86**, 155424 (2012); *New J. Phys.* **15**, 013014 (2013).
  - [33] L. Simine and D. Segal, *arXiv* 1302.5761.
  - [34] L. Simine and D. Segal, *Phys. Chem. Chem. Phys.* **14**, 13820 (2012).
  - [35] D. Segal, *Phys. Rev. B* **73**, 205415 (2005).
  - [36] B. N. J. Persson and H. Ueba, *Phys. Rev. B* **76**, 125401 (2007).
  - [37] D. Segal and A. Nitzan, *Phys. Rev. Lett.* **94**, 034301 (2005); *J. Chem. Phys.* **122**, 194704 (2005).
  - [38] L. Nicolin and D. Segal, *J. Chem. Phys.* **135**, 164106 (2011).
  - [39] B. Roulet, J. Gavoret, and P. Nozieres, *Phys. Rev.* **178**, 1072 (1969); P. Nozieres and C. T. D. Dominicis, **178**, 1097 (1969).
  - [40] T.-K. Ng, *Phys. Rev. B* **54**, 5814 (1996).
  - [41] K. L. Hur, "Understanding quantum phase transitions," (Taylor and Francis, Boca Raton, 2010).
  - [42] M. M. J. T. Muhonen and J. P. Pekola, *Rep. Prog. Phys.* **75**, 046501 (2012).
  - [43] M. Esposito, K. Lindenberg, and C. V. den Broeck, *Euro. Phys. Lett.* **85**, 60010 (2009).
  - [44] R. P. Feynman and A. R. Hibbs, *Quantum Mechanics and Path Integrals* (McGraw-Hill, New-York, 1965).